

# Intracardiac flow separation in an *in situ* perfused heart from Burmese python *Python molurus*

Tobias Wang<sup>1,\*</sup>, Jordi Altimiras<sup>2</sup> and Michael Axelsson<sup>2</sup>

<sup>1</sup>Department of Zoophysiology, University of Aarhus, 8000 Aarhus C, Denmark and <sup>2</sup>Department of Zoophysiology, University of Gothenburg, Sweden

\*Author for correspondence (e-mail: tobias.wang@biology.au.dk)

Accepted 6 June 2002

## Summary

The heart of non-crocodilian reptiles has two separate atria that receive blood from the systemic and pulmonary circulations. The ventricle is not fully divided, but is compartmentalised into two chambers (cavum dorsale and cavum pulmonale) by a muscular ridge that runs from the apex to the base of the ventricle. The muscular ridge is small in turtles, but is well developed in varanid lizards and many species of snakes. These anatomical differences correlate with an effective blood flow separation in varanid lizards, whereas turtles can exhibit very large cardiac shunts. Very little is known about the cardiac shunt patterns in other groups of reptiles.

Here we characterise cardiac performance and flow dynamics in the Burmese python (*Python molurus*) using an *in situ* perfused heart preparation. The pericardium remained intact and the two atria were perfused separately (Ringer solution), and the two systemic and the pulmonary outflows were independently cannulated. Right and left atrial filling pressures and ventricular outflow pressures of the pulmonary and systemic vessels could be manipulated independently, permitting the establishment of large experimental intraventricular pressure gradients across the muscular ridge. The maximal power output

generated by the systemic side of the ventricle exceeded the maximal power output that was generated by the cavum pulmonale that perfuse the pulmonary circulation. Furthermore, systemic flow could be generated against a higher outflow pressure than pulmonary flow. Perfusate entering the right atrium was preferentially distributed into the pulmonary circulation, whereas perfusate into the left atrium was distributed to the systemic circulation.

Our study indicates that the well-developed muscular ridge can separate the cavum systemic and pulmonary sides of the heart to prevent mixing of systemic and pulmonary flows. Therefore, the heart of *Python* appears to exhibit a large degree of ventricular flow separation as previously described for varanid lizards. We speculate that the ventricular separation has evolved in response to the need of maintaining high oxygen delivery while protecting the pulmonary circulation from oedema as result of high vascular pressures.

Key words: reptile, snake, python, *Python molurus*, cardiovascular, perfused heart, blood flow, filling pressure, Starling curve, power curve, cardiac shunting.

## Introduction

The heart of non-crocodilian reptiles has two atria supplying the ventricle from the systemic and pulmonary circulations. The ventricle is not fully divided, but is compartmentalised into the cavum dorsale and the cavum pulmonale by a muscular ridge that runs from the apex to the base of the ventricle (Webb, 1979; Johansen and Burggren, 1980; van Mierop and Kutsche, 1985; Hicks, 1998). The cavum dorsale is further divided into the cavum arteriosum (CA) and the cavum venosum (CV). The pulmonary artery emerges from the cavum pulmonale (CP) while the left and right aortic arches (LAo and RAo, respectively) emerge from the CV. During ventricular diastole, oxygen-poor blood from the right atrium (RA<sub>t</sub>) enters the CV and flows across the muscular ridge to enter the CP, while oxygen-rich blood from the left atrium directly fills the CA.

Oxygen-poor blood that remains within the CV by onset of ventricular systole will be recirculated into the systemic circulation (right-to-left shunt), whereas oxygen-rich blood that may remain at this site by the start of ventricular diastole can be carried to the CP and recirculated into the pulmonary circulation (left-to-right shunt). This mechanism is normally referred to as 'wash-out shunt' and its magnitude depends on end-systolic and end-diastolic volumes of CV relative to CP and CA. These volumes are, in turn, affected by cardiac contractility as well as pre- and afterloads (Heisler and Glass, 1985). In addition to the wash-out shunt, blood can be shunted between the CP and the CA during ventricular systole if the muscular ridge fails to separate these chambers (Heisler and Glass, 1985; Hicks and Malvin, 1995). The magnitude of this

'pressure shunt' depends on the opening between the chambers and the pressure difference between them, which is determined by cardiac contractility and the outflow resistances in the pulmonary and systemic circulations (Johansen and Burggren, 1980; Heisler and Glass, 1985; Hicks, 1998). Therefore, the power development and contractility of the heart as well as pre- and afterloads are potential determinants of cardiac shunt patterns in non-crocodylian reptiles.

Wash-out and pressure shunts can occur simultaneously in a given species (e.g. Hicks et al., 1996; Hicks, 1998), but their relative contribution may depend on the size of the muscular ridge, cardiac contractility and the size of the CV (Heisler and Glass, 1985). Turtles can exhibit large cardiac shunts, which correlate with a small muscular ridge that is unable to separate pressures between the ventricular chambers (e.g. Shelton and Burggren, 1976). Thus, a pressure shunt is probably the most important mechanism (Shelton and Burggren, 1976; Hicks et al., 1996). In contrast, the CV of varanid lizards is greatly reduced and they possess a very well developed muscular ridge (e.g. Webb, 1979). The large muscular ridge separates the CP from the CA early in ventricular systole and allows for much higher pressures in CA compared with CP, as well as an effective separation of intraventricular blood flows (Burggren and Johansen, 1982; Heisler et al., 1983). Varanid lizards sustain the highest metabolic rates of any reptile during exercise and it has been suggested that there is a correlation between the ability to separate ventricular blood flows and the metabolic rate (see Wang and Hicks, 1996; Wang et al., 2001c).

Ventricular shunt patterns have not been thoroughly investigated in many species of non-crocodylian reptiles, so the extent to which different species can separate blood flows is not well known (e.g. Hicks, 1998). Several anatomical descriptions of *Python* have shown a very well developed muscular ridge as well as a reduced CV, and the cardiac anatomy of pythons resembles that of varanid lizards (Webb, 1979; van Mierop and Kutsche, 1985; Farrell et al., 1998). It seems likely, therefore, that the heart of *Python* can exert considerable flow separation. Consistent with this possibility, pythons can sustain high rates of oxygen consumption over several days when they digest large meals (e.g. Secor and Diamond, 1995). Therefore, we decided to investigate cardiac performance and flow dynamics in the Burmese python, *Python molurus*. For this purpose, we used an *in situ* perfused heart, which allowed for separate control of the input and output pressures (preload and afterload, respectively).

### Materials and methods

The experiments were performed on an *in situ* perfused heart preparation similar to that described previously by Franklin and Axelsson (1994). The pericardium remained intact and the heart was perfused by a Ringer solution, through the two atria, while the two systemic arteries and the common pulmonary artery were independently cannulated. Atrial filling pressures and pulmonary and systemic outflow pressures could, therefore, be manipulated independently.

### Experimental animals

The study was conducted on seven specimens of Burmese pythons (*Python molurus*, L.) with a body mass of 1.5–3.3 kg ( $2.2 \pm 0.2$  kg, mean  $\pm$  s.e.m.). These snakes were bred in captivity and were transported to Gothenburg 1 week before the experiments began. Here they were kept in individual chambers at 30 °C with free access to water and a 12 h:12 h L:D cycle.

### Surgery and instrumentation for the perfused heart preparation

The snakes were anaesthetised with an intraperitoneal injection of 15–20 mg kg<sup>-1</sup> sodium pentobarbital and the surgery was started as soon as the responses to pinching of the skin had ceased. The lungs were artificially ventilated (97% O<sub>2</sub>, 3% CO<sub>2</sub>) during instrumentation to maintain oxygenation of the heart, and blood coagulation was prevented by a systemic injection of heparin (2000 IU kg<sup>-1</sup>).

To cannulate the central blood vessels, the abdomen was opened by a ventral incision. The left atrium was accessed through the common pulmonary vein that drains both lungs, whereas the right atrium was accessed through the hepatic vein; all other systemic veins were ligated. Both the right aortic arch (RAo) and the left aortic arch (LAo) were cannulated, and these outflows were joined by a T-piece so that total systemic outflow could be measured in one common outflow. The carotid and vertebral arteries were ligated. The pulmonary outflow was collected from the larger right pulmonary artery, whereas the left pulmonary artery was ligated. When all the catheters were in place, the head and the rostral portion of the snake was cut and the *in situ* perfused heart was placed in a thermostat-controlled bath, maintained at 30 °C, containing a Ringer solution that resembles normal plasma composition (Overgaard et al., 1999). The Ringer had the following composition (in mmol l<sup>-1</sup>): NaCl, 115; KCl, 2.5; MgSO<sub>4</sub>·7H<sub>2</sub>O, 1; CaCl<sub>2</sub>·2H<sub>2</sub>O, 2.5; NaHCO<sub>3</sub>, 24.8; NaH<sub>2</sub>PO<sub>4</sub>, 1.2; Hepes, 10; glucose, 5; and pyruvate, 5. Polyvinylpyrrolidone (PVP; 3%) was added as a volume expander. The solution was adjusted to pH 7.5 with NaOH at a P<sub>CO<sub>2</sub></sub> of 3 kPa. The perfusion of the heart was started immediately after completing the surgery and the preparation was allowed to stabilise for 20 min.

All cannulations were performed with double-bore stainless steel cannulae (see Franklin and Axelsson, 1994), so pressures could be measured at the tip of insertion. The in- and outflow pressures were measured with four DPT-6100 (Peter von Berg) pressure transducers, that were calibrated daily against static water columns. The systemic and pulmonary outflows (Q<sub>sys</sub> and Q<sub>pul</sub>, respectively) were measured by two 4NRB flow probes (Transonic System, Ithaca, NY, USA) placed in the outflow tracts and connected to a Transonic T206 flow meter. The pressure transducers and the flow meter were connected to a Grass 7G Polygraph for appropriate amplification and filtering. Heart rate was derived from the pulsatile pressures using a Grass tachograph (Model 7P44D) and all signals were recorded on-line by a LabView 5.1 (National Instrument) data-acquisition system.

Table 1. *Haemodynamic variables for the in situ perfused Python molurus heart*

Body mass ( $B_M$ )	2.2±0.2 kg
Ventricular mass ( $V_M$ )	3.61±0.46 g
Pressure in left atrium ( $P_{LA_t}$ )	0.20±0.02 kPa
Pressure in right atrium ( $P_{RA_t}$ )	0.11±0.01 kPa
Systemic arterial pressure ( $P_{sys}$ )	6.3±0.0 kPa
Pulmonary arterial pressure ( $P_{pul}$ )	6.3±0.1 kPa
Heart rate ( $f_H$ )	46±3 min <sup>-1</sup>
Systemic flow ( $\dot{Q}_{sys}$ )	12.0±0.7 ml min <sup>-1</sup> kg <sup>-1</sup>
Pulmonary flow ( $\dot{Q}_{pul}$ )	12.8±0.9 ml min <sup>-1</sup> kg <sup>-1</sup>
Cardiac output ( $\dot{Q}_{tot}$ )	24.7±1.6 ml min <sup>-1</sup> kg <sup>-1</sup>
Total stroke volume ( $V_S$ )	0.55±0.05 ml kg <sup>-1</sup>
Systemic power output	1.22±0.07 mW kg <sup>-1</sup>
Pulmonary power output	1.32±0.09 mW kg <sup>-1</sup>
Total power output	2.53±0.15 mW kg <sup>-1</sup> body mass
Total power output	1.60±0.15 mW g <sup>-1</sup> ventricular mass

These conditions were used as starting conditions in all experimental protocols and were attained by adjusting filling pressures of the two atria ( $P_{RA_t}$  and  $P_{LA_t}$ ) so that the  $\dot{Q}_{sys}$  and  $\dot{Q}_{pul}$  were equal at 12–13 ml min<sup>-1</sup> kg<sup>-1</sup>. Values are means ± S.E.M. ( $N=7$ ).

### Experimental protocols

The outflow pressures in both the systemic and pulmonary circulations were set at 6.5 kPa to mimic the systemic blood pressure in the closely related *Boa constrictor* (Wang et al., 2001b) and anaesthetised pythons (Wang et al., 2000) ( $P_{sys}$  and  $P_{pul}$  have not been previously reported for unanaesthetised pythons). The filling pressures were then adjusted to attain a total cardiac output (i.e.  $\dot{Q}_{sys} + \dot{Q}_{pul}$ ) of approximately 25 ml min<sup>-1</sup> kg<sup>-1</sup> that was distributed evenly between the two circuits (Table 1). This resulted in a  $\dot{Q}_{sys}$  of 12 ml min<sup>-1</sup> kg<sup>-1</sup>, which is lower than the systemic blood flow of 19 ml min<sup>-1</sup> kg<sup>-1</sup> that has been measured *in vivo* during resting conditions in *P. molurus* (Secor et al., 2000). Having adjusted the filling pressures and allowed the flows to stabilise, three experimental protocols were performed in the following order:

#### (1) Effects of altering filling pressures: Starling curves

To quantify the influence of filling pressure on stroke volume and cardiac output, the input pressure was varied at constant output pressures (6.5 kPa). The filling pressures of the left and right atria were manipulated independently. The experiments were started by lowering the left atrial filling pressure until systemic flow had decreased to around 25 % of the control condition. Then, filling pressure was increased in steps of approximately 0.05 kPa to a maximum value of approximately 0.7 kPa. Flows and pressures stabilised within 15 s at each level and a subsequent 15 s recording was used for data analysis. After completion of the Starling curve from the left atrium, filling pressure to the right atrium was lowered until pulmonary flow decreased to approximately 25 % of the control value. Preload to the right atrium was then increased

in steps of 0.05 kPa until a maximum pressure of 0.4 kPa was reached.

#### (2) Effects of altering output pressures

Filling pressures were readjusted to attain control level flows at output pressures of 6.5 kPa. Then, output pressure of the systemic or the pulmonary circulation was reduced abruptly to 1 kPa followed by stepwise increases (1 kPa for each step) until an outflow pressure of 13 kPa was reached for the systemic side. Because flow in the pulmonary side was more sensitive to increases in outflow pressure, it was only increased to 9 kPa on this side. During these experiments the output pressure in the other circuit remained constant at 6.5 kPa.

#### (3) Effects of atrial input occlusion and output pressures

To test for intracardiac pressure and flow separation the outflow pressure of the pulmonary and systemic side of the heart were altered simultaneously and independently. During these manipulations, constant input pressures were maintained. In the control situation the output pressures of the systemic and pulmonary circuits were independently varied to levels of 3.0, 6.5 and 8.0 kPa in randomly chosen combinations. Following this protocol, we repeated these manipulations after having clamped one of the two atrial inflows. Thus, when standard flow conditions were achieved, the inflow to one atrium was clamped by a haemostat on the inflow cannula, and flows were allowed to stabilise. Then the output pressures of the systemic and pulmonary circuits were varied as described for the control experiments above. Finally, the inflow to the other atrium was clamped and the changes in outflow pressure were repeated. Flows and pressures stabilised within 15 s at each combination of outflow pressures and the steady flows occurring over the subsequent 15 s period were used for data analysis.

#### Calculation of haemodynamic variables, cardiac work and statistics

Heart rate ( $f_H$ ) was derived from the pulsatile flow signal, and stroke volumes ( $V_S$ ) were calculated for the systemic (left and right aortic outflow combined) and pulmonary outflow separately as flow/ $f_H$ . Flows and stroke volumes were normalised per gram ventricle. Flows from the left and right aortic arches ( $\dot{Q}_{LA_o}$  and  $\dot{Q}_{RA_o}$ , respectively) were combined to give total systemic flow (i.e.  $\dot{Q}_{sys} = \dot{Q}_{LA_o} + \dot{Q}_{RA_o}$ ). Cardiac power output (mW) was also calculated separately for the systemic and pulmonary output using the following equations:

$$\text{Systemic power output range} = [(P_{sys} - P_{LA_t}) \times \dot{Q}_{sys}] \times 0.0167, \quad (1)$$

$$\text{Pulmonary power output} = [(P_{pul} - P_{LA_t}) \times \dot{Q}_{pul}] \times 0.0167, \quad (2)$$

$$\text{Total cardiac power} = \text{Systemic power output} + \text{Pulmonary power output}, \quad (3)$$

where  $\dot{Q}_{sys}$  and  $\dot{Q}_{pul}$  are systemic and pulmonary flows (ml min<sup>-1</sup>), respectively;  $P_{sys}$  and  $P_{pul}$  are systemic and pulmonary outflow pressures (kPa), respectively;  $P_{RA_t}$  and

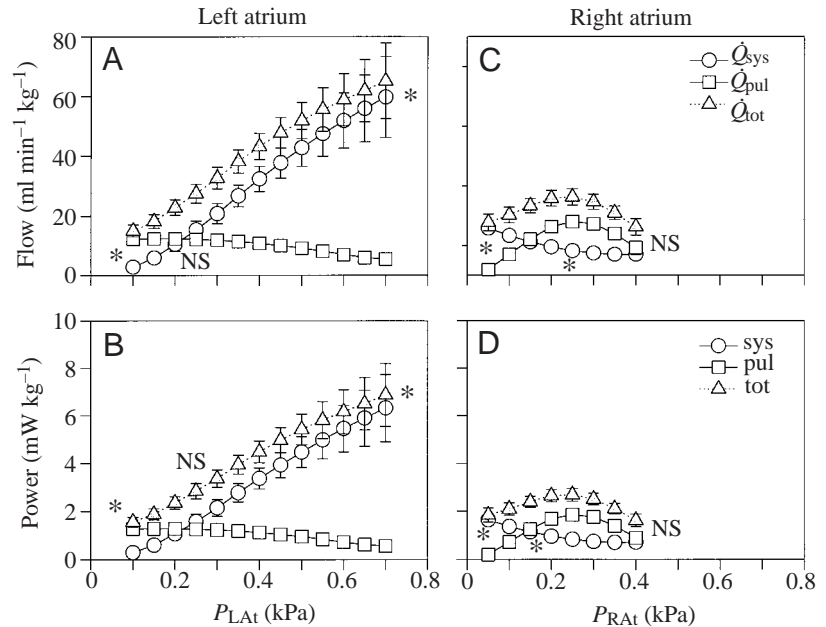


Fig. 1. Effects of increasing input pressure  $P_{LA_t}$  and  $P_{RA_t}$  (Frank–Starling effect) to the left atrium (LAT: A,B) or right atrium (RAT: C,D) on central flow rates  $\dot{Q}$  (A,C) and power output (B,D) in *Python molurus* heart. In each of the two cases, input pressure to the other atrium was maintained constant. All values are means  $\pm$  S.E.M. ( $N=7$ ); an asterisk indicates significant differences ( $P<0.05$ ) between systemic or pulmonary flow rates and power outputs at a given input pressure. NS, not significantly different; sys, systemic; pul, pulmonary; tot, total.

$P_{LA_t}$  are the input pressures in the right and left atria (kPa), respectively; and 0.0167 is a conversion factor for mW ( $=1/60$ , to convert flow from  $\text{ml min}^{-1}$  to  $\text{ml s}^{-1}$ ).

Total cardiac power output for the whole heart was normalised to heart mass. However, it was not possible to estimate the mass of the subcompartments in the undivided ventricle and power output for the systemic and pulmonary outflow were, therefore, normalised to body mass. For each individual animal, flow and power were fitted to filling pressure and output pressure using a third-order polynomial function. The individual polynomial equations were used to generate data at set pressure (input or output) intervals, so that pre-load data points could be generated in 0.05 kPa steps, whereas afterload curves were generated for each 0.5 kPa step. Finally, these individual fits were combined to produce composite graphs consisting of means of all animals.

All data are presented as means  $\pm$  S.E.M. ( $N=7$ ). A Wilcoxon's sign rank test for matched pairs was used to test for significant changes. For protocols 1 and 2 we tested for significant differences between  $\dot{Q}_{\text{sys}}$  and  $\dot{Q}_{\text{pul}}$  or Power from the systemic side and Power from the pulmonary side. This was done only at three points in the curves, the lowest and the highest pressures tested and an intermediate pressure. For protocol 3 we tested for differences in  $\dot{Q}_{\text{sys}}$  before and after clamping. Statistical significance was set at  $P<0.05$ .

## Results

Table 1 shows the baseline haemodynamic variables of the *in situ* perfused *Python* heart, where the outflow pressures were set at 6.5 kPa and the inflow pressures were adjusted so that the total cardiac output was  $24.7 \pm 1.6 \text{ ml kg}^{-1} \text{ min}^{-1}$ . The heart rate during these conditions was stable at a mean value of  $46 \pm 3 \text{ min}^{-1}$  and total stroke volume averaged

$0.55 \pm 0.05 \text{ ml kg}^{-1}$  (Table 1). These baseline values were attained before each experimental protocol.

The effects of independently altering the filling pressures to the two atria on flow and power development are presented as Starling curves in Fig. 1. Filling of the left atrium, which receives pulmonary venous blood *in vivo*, markedly increased  $\dot{Q}_{\text{sys}}$ , whereas  $\dot{Q}_{\text{pul}}$  decreased (Fig. 1A). Although left atrial filling pressure was elevated to 0.7 kPa,  $\dot{Q}_{\text{sys}}$  did not appear to reach a plateau during the experiments. Filling of the right atrium, which receives systemic oxygen-poor blood *in vivo*, resulted in maximal  $\dot{Q}_{\text{pul}}$  and power development at values between 0.2 and 0.3 kPa. Increasing filling pressure of the right atrium led to a small decrease in  $\dot{Q}_{\text{sys}}$ . Because output pressure was kept constant, the power output during filling of the left or the right atrium mirrored the changes in flows (Fig. 1B,D).

Fig. 2 depicts the effects of increasing outflow pressure, at constant inflow pressure, on flow and power output. In these experiments, outflow pressure was either altered in the systemic or pulmonary circulation (Fig. 2A,B and C,D, respectively). For both the systemic and pulmonary circulation, increased outflow pressure caused a progressive decline in flow to that side of the circulation (Fig. 2A,C). Flow in the other side of the heart was also affected, but the absolute changes were smaller. Increased outflow pressure in the systemic arches ( $P_{\text{sys}}$ ) caused a small increase in  $\dot{Q}_{\text{pul}}$  from  $8.6 \pm 2.0$  to  $12.2 \pm 0.5 \text{ ml kg}^{-1} \text{ min}^{-1}$ , but further increase above 6 kPa caused a decline in  $\dot{Q}_{\text{pul}}$  to a value of around  $5.4 \pm 1.5 \text{ ml kg}^{-1} \text{ min}^{-1}$  (Fig. 2A). Increasing the outflow pressures in the pulmonary circulation from 1 to 9 kPa, caused a decline of  $\dot{Q}_{\text{pul}}$  from  $31.5 \pm 4.4$  to  $0 \text{ ml kg}^{-1} \text{ min}^{-1}$  and was associated with a reduction in  $\dot{Q}_{\text{sys}}$  from  $23.0 \pm 3.2$  to  $10.2 \pm 1.6 \text{ ml min}^{-1} \text{ kg}^{-1}$ . As noted for the Starling curves, there were substantial differences between the systemic and pulmonary circulation. Most strikingly, an increase in the outflow pressure to 9 kPa completely abated  $\dot{Q}_{\text{pul}}$ , whereas  $\dot{Q}_{\text{sys}}$

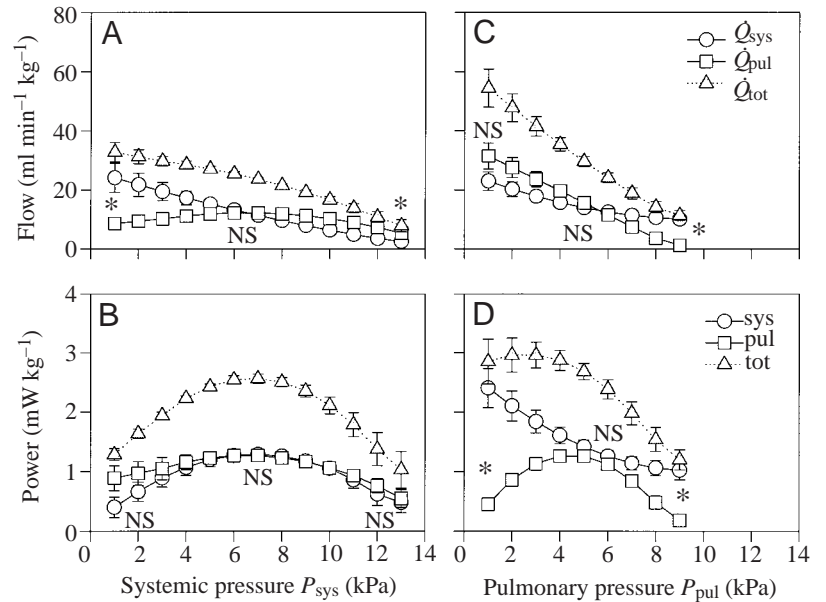


Fig. 2. Effects of increasing output pressure (power curves) of the systemic (A,B) or pulmonary (C,D) outflows on central flows (A,C) and power output (B,D) of the *in situ* perfused *Python molurus* heart. In each case, output pressure of the other circulatory system was maintained at a constant level. All values are means  $\pm$  S.E.M. ( $N=7$ ); an asterisk indicates significant differences ( $P<0.05$ ) between systemic or pulmonary flows and power outputs at a given outflow pressure. NS, not significantly different; sys, systemic; pul, pulmonary; tot, total.

Table 2. Absolute systemic ( $\dot{Q}_{\text{sys}}$ ) and pulmonary ( $\dot{Q}_{\text{pul}}$ ) flows during the experimental clamping of the systemic vein (right atrial inflow) or pulmonary vein (left atrial inflow)

	$P_{\text{sys}}=3 \text{ kPa}$		$P_{\text{sys}}=6.5 \text{ kPa}$		$P_{\text{sys}}=8 \text{ kPa}$	
	$\dot{Q}_{\text{sys}}$	$\dot{Q}_{\text{pul}}$	$\dot{Q}_{\text{sys}}$	$\dot{Q}_{\text{pul}}$	$\dot{Q}_{\text{sys}}$	$\dot{Q}_{\text{pul}}$
$P_{\text{pul}}=8 \text{ kPa}$						
Control	19.3 $\pm$ 3.1*	2.1 $\pm$ 0.9	9.9 $\pm$ 1.6*	4.0 $\pm$ 1.1		
Clamp systemic vein						
Clamp pulmonary vein	12.3 $\pm$ 3.2 $^{\dagger,*}$	1.7 $\pm$ 0.7	4.9 $\pm$ 1.5 $^{\dagger}$	2.6 $\pm$ 0.7		
$P_{\text{pul}}=6.5 \text{ kPa}$						
Control	20.5 $\pm$ 3.7*	7.3 $\pm$ 1.5	11.4 $\pm$ 1.2	11.1 $\pm$ 0.7	7.3 $\pm$ 1.5	9.4 $\pm$ 0.6
Clamp systemic vein	25.3 $\pm$ 2.8*	0.4 $\pm$ 0.3 $^{\dagger}$	16.9 $\pm$ 2.2 $^{\dagger,*}$	0.6 $\pm$ 0.4 $^{\dagger}$	13.8 $\pm$ 1.2*	0.4 $\pm$ 0.3 $^{\dagger}$
Clamp pulmonary vein	10.6 $\pm$ 3.4 $^{\dagger}$	5.2 $\pm$ 1.4	2.7 $\pm$ 1.0 $^{\dagger,*}$	10.2 $\pm$ 1.5		
$P_{\text{pul}}=3 \text{ kPa}$						
Control	24.7 $\pm$ 2.3	27.9 $\pm$ 3.8	17.6 $\pm$ 1.8	27.2 $\pm$ 3.7	13.3 $\pm$ 2.0*	25.3 $\pm$ 3.5
Clamp systemic vein	30.5 $\pm$ 4.1*	2.1 $\pm$ 0.7 $^{\dagger}$	23.7 $\pm$ 2.5*	3.6 $\pm$ 0.6 $^{\dagger}$	19.9 $\pm$ 1.8*	3.8 $\pm$ 0.6 $^{\dagger}$
Clamp pulmonary vein	4.4 $\pm$ 2.2 $^{\dagger,*}$	28.5 $\pm$ 3.3	1.7 $\pm$ 0.9 $^{\dagger,*}$	29.9 $\pm$ 2.9		

Values are presented as means  $\pm$  S.E.M. ( $N=7$ ).

$P_{\text{sys}}$ , systemic arterial pressure;  $P_{\text{pul}}$ , pulmonary arterial pressure.

\*Significant difference between  $\dot{Q}_{\text{sys}}$  and  $\dot{Q}_{\text{pul}}$ .

$^{\dagger}$ Significant difference between the control condition and the clamping condition.

was  $8 \text{ ml kg}^{-1} \text{ min}^{-1}$  (a reduction of two-thirds compared with the lowest outflow resistance) at a similar  $P_{\text{sys}}$ . Furthermore,  $\dot{Q}_{\text{sys}}$  persisted even at the maximal tested outflow pressure of 13 kPa.

The changes in systemic and pulmonary flows from experimental protocol 3 are presented in Table 2. Flows are expressed relative to total cardiac output (i.e.  $\dot{Q}_{\text{pul}}+\dot{Q}_{\text{sys}}$ ) in Figs 3 and 4, where the left-hand panels show the data obtained when only outflow pressures were manipulated, while the right-hand panels show the flows measured with alteration of output pressures following occlusion of the input to one of the

atria. The effects of manipulating one of outflow pressures ( $P_{\text{sys}}$  or  $P_{\text{pul}}$ ; see Table 2) were similar to the data presented in Fig. 2. Thus,  $\dot{Q}_{\text{sys}}$  gradually decreased when  $P_{\text{sys}}$  was increased, while only small changes occurred in  $\dot{Q}_{\text{pul}}$  (Table 2). By contrast, changes in  $P_{\text{sys}}$  predominantly affected  $\dot{Q}_{\text{pul}}$  (Table 2). These findings indicate that the flows entering the heart from the two atria are functionally separated. This was investigated further by clamping the inflow to one of the atria and repeating the changes in outflow pressures (right-hand panels in Figs 3, 4; Table 2). When the systemic vein was clamped at baseline conditions (Table 1),  $\dot{Q}_{\text{pul}}$  decreased

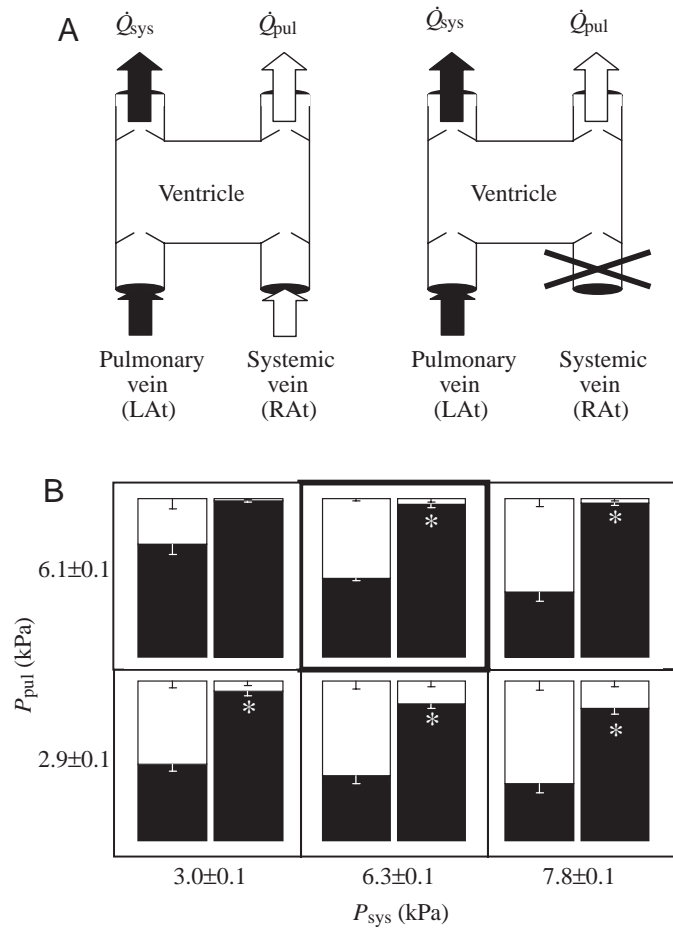


Fig. 3. Effects of independently changing outflow resistances in the pulmonary and systemic circulations on flow distributions before and after clamping the inflow to the right atrium (RA; A). (B) The left bar in each panel shows the flow distribution during filling of both atria, whereas the right bars show the distribution when right atrial flow was completely abolished. The starting condition is marked by a thicker border; black bars, pulmonary vein; white bars, systemic vein. All values are means  $\pm$  S.E.M. ( $N=7$ ); an asterisk indicates a significant effect ( $P < 0.05$ ) from clamping atrial inflow. LAt, left atrium.

from  $11.1 \pm 0.7 \text{ ml min}^{-1} \text{ kg}^{-1}$  to  $0.6 \pm 0.4 \text{ ml min}^{-1} \text{ kg}^{-1}$  (Fig. 3; Table 2). Similarly, when the pulmonary vein was clamped, there was a large reduction in  $\dot{Q}_{sys}$  (from  $11.4 \pm 1.2 \text{ ml min}^{-1} \text{ kg}^{-1}$  to  $2.7 \pm 1.0 \text{ ml min}^{-1} \text{ kg}^{-1}$ ) (Fig. 4; Table 2). These patterns applied to all combinations of outflow pressures, and flow distributions were invariably affected by clamping one of the inflow to the atria (Figs 2, 4). However, the pulmonary circulation was less affected by atrial clamping than the systemic circulation. In both cases, the amount of perfusate that was shunted to the other circulatory system increased with the difference between outflow pressures. During clamping of the systemic vein, the maximal amount of shunted perfusate was  $17 \pm 4\%$  and occurred at  $P_{pul}/P_{sys}$  of 3 kPa/8 kPa (Fig. 3), whereas the maximal shunt during clamping of the pulmonary vein was  $83 \pm 8\%$  and occurred at a  $P_{pul}/P_{sys}$  of 8 kPa/3 kPa (Fig. 4).

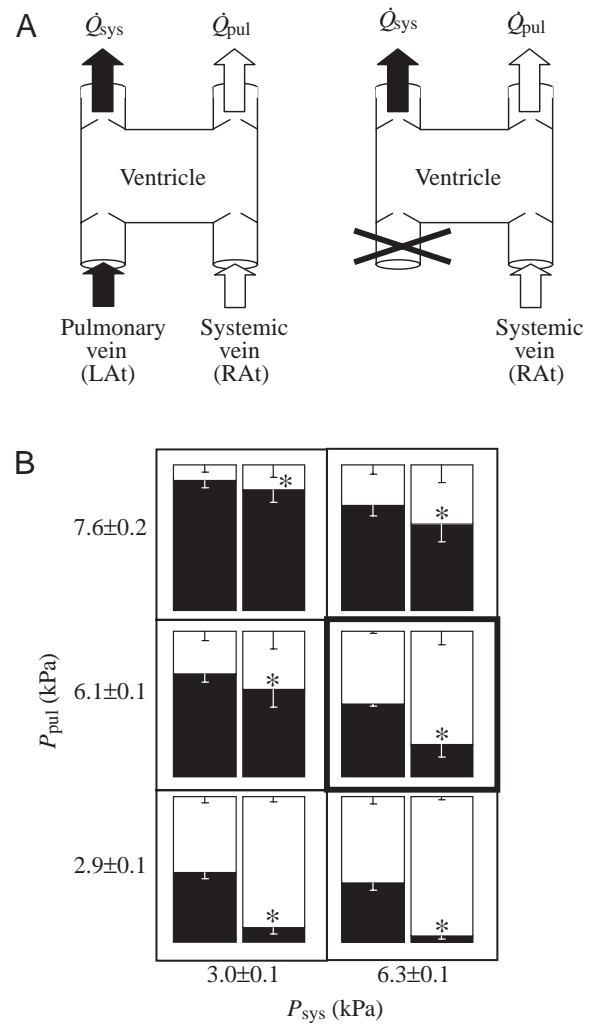


Fig. 4. Effects of independently changing outflow resistances in the pulmonary and systemic circulations on flow distributions before and after clamping the pulmonary vein (left atrial inflow) (LAt; A). (B) The left bar in each panel shows the flow distribution during filling of both atria, whereas the right bars show the distribution when right atrial flow was completely abolished. The starting condition is marked by a thicker border; black bars, pulmonary vein; white bars, systemic vein. All values are means  $\pm$  S.E.M. ( $N=7$ ); an asterisk indicates a significant effect ( $P < 0.05$ ) from clamping atrial inflow.

### Discussion

The present study shows pronounced differences between the systemic and the pulmonary sides of the ventricle in the *in situ* perfused heart of *Python molurus*. Thus, the cavum arteriosum, which supplies the systemic circulation, can generate flows against higher maximal pressures and can sustain higher power generation than the cavum pulmonale that supplies the pulmonary circulation (Figs 1, 2). These differences are coupled with a considerable degree of flow separation between the systemic and pulmonary circulations (Figs 3, 4). The large degree of flow separation resembles previous descriptions in varanid lizards and indicates that

functional ventricular flow and pressure separation may be more widespread among non-crocodilian reptiles than previously recognised.

*Differential power and Starling curves for the cavum arteriosum and the cavum pulmonale*

Stroke volume was very sensitive to filling pressure and the *in situ* perfused *P. molurus* heart exhibited a marked Frank–Starling response as previously shown for turtles, crocodiles and other vertebrates (Reeves, 1963; Strobeck and Sonnenblick, 1986; Farrell et al., 1992; Farrell et al., 1994; Franklin, 1994; Franklin and Axelsson, 1994). There was no effect of increased filling pressure on heart rate (data not shown). This is also the case in turtles (Farrell et al., 1994; Franklin, 1994), whereas filling of the right atrium exerts a chronotropic effect in crocodiles (Franklin and Axelsson, 1994). This response can probably be ascribed to excitement of the sinoatrial pacemaker by stretch of the atrial wall. In mammals, approximately 15% of the increased heart rate following increased atrial pressure is due to stretch of the S-A node, and the rest to the Bainbridge effect (Guyton, 1986). Our data suggest that atrial stretch receptors are of little importance in modulating the pacemaker in *P. molurus*.

Our experiments show that the systemic and pulmonary sides of the *P. molurus* heart exhibit very different quantitative responses to changes in filling and outflow pressures. Thus, the maximal power output from the cavum arteriosum, which perfuses the systemic circulation *in vivo*, is at least threefold higher than the power output from the cavum pulmonale, which perfuses the pulmonary circulation (Figs 1, 2). This indicates that the strength of contraction in the cavum arteriosum greatly exceed that in the cavum pulmonale. The differences in power development between the two sides of the ventricle are reflected in the ability to generate flows against elevated resistance in the outflow tracts.  $\dot{Q}_{pul}$  ceased when outflow pressure in the pulmonary artery was increased to approximately 9 kPa, while the systemic side of the heart was able to deliver a flow against no less than 13 kPa (Fig. 2). Thus, the cavum arteriosum was able to maintain systemic flow in the face of increased systemic outflow pressure to a larger degree than the cavum pulmonale. Differences in the contractile properties of the cavum arteriosum versus the cavum pulmonale have been previously proposed by Farrell et al. (1998), who noted that the ventricular wall surrounding the CA is much thicker than the wall surrounding the CP (Farrell et al., 1998).

The larger power generating ability of the CA compared with the CP of the perfused *P. molurus* heart indicates that systemic blood pressure can greatly exceed pulmonary pressures *in vivo*. Systemic blood pressure can indeed exceed 20 kPa during forced activity in *Boa constrictor* (Wang et al., 2001a) and immediately following induction of anaesthesia in *P. regius* (T. W. and M. A., unpublished), but pulmonary blood pressures have not been reported. Ventricular pressure separation has not been demonstrated in other snakes. *Vipera berus* and *Natrix natrix* exhibit identical systolic pressures in

systemic and pulmonary arteries and ventricular pressures showed no indication of pressure separation (Johansen, 1959). In *Thamnophis* spp., the pressures in the pulmonary artery are lower than systemic pressures, but there were no intraventricular pressure differences and the lower pulmonary pressure can be explained by constriction of a muscle surrounding the base of the pulmonary artery (Burggren, 1977). Clearly, intraventricular pressures need to be measured in *P. molurus* to investigate whether their heart differs from the other snakes. Within non-crocodilian reptiles, a clear pressure separation between the pulmonary and systemic circulations has so far been established only for varanid lizards (e.g. Millard and Johansen, 1974; Heisler et al., 1983) and may be related to the ability of these lizards to maintain high aerobic metabolism during exercise (Wang and Hicks, 1996).

*Separation of blood flows and ventricular shunts in the perfused P. molurus heart*

The different power relationships of the CP and CA were associated with an apparent ability to separate flows entering the ventricle from the two atria. Thus, increased filling of the right atrium preferentially affected  $\dot{Q}_{pul}$ , and  $\dot{Q}_{sys}$  was only marginally affected when the outflow pressure was elevated in the pulmonary artery. A reciprocal relationship was observed for the other side of the heart (Figs 3, 4). Therefore, it appears that perfusate entering the *in situ* perfused heart from the two atria are well separated during both ventricular diastole and systole. The separation of flows during diastole is likely to be caused by the atrio–ventricular valves that direct right atrial inflow across the muscular ridge to the PA, while the other valve directs left atrial perfusate into the base of the CA (see White, 1968; Webb, 1979). Early in ventricular systole, the flow separation between the CA and CP is probably accomplished by the well-developed muscular ridge in *P. molurus* (Farrell et al., 1998). If the muscular ridge does indeed separate the CA and CP during systole, this would allow for differential pressures within the chambers, as observed in *Varanus exanthematicus* (Burggren and Johansen, 1982).

The apparent separation of flows within the ventricle was further substantiated from the experiments where atrial inflows were clamped (Figs 3, 4). Clamping of the right atrium virtually abolished  $\dot{Q}_{pul}$  even when  $P_{pul}$  was set much lower than  $P_{sys}$  (Fig. 3). These experiments show that virtually all the perfusate delivered to the caudal portion of the CA from the left atrium remains there during the entire diastolic phase and is virtually incapable of crossing the muscular ridge to enter the CP. This separation persisted when  $P_{pul}$  was reduced substantially compared to  $P_{sys}$ . Thus, the extent to which intraventricular pressure differences can affect L–R shunt (recirculation of pulmonary venous blood to the lungs) appears to be very small.

Clamping the left atrium caused substantial reduction in  $\dot{Q}_{sys}$ , but some of the perfusate entering the right atrium was ejected through the systemic arches when  $P_{pul}$  was set high.

Under these circumstances, some of the perfusate that enters the CV during diastole does not cross the muscular ridge, and instead enters the CA and is ejected through the systemic arteries (equivalent of R–L shunt). Furthermore, because the CP is weaker than the CA, contraction of the CP may be unable to overcome high pulmonary pressures and end-systolic volume of the CP is likely to be high during these conditions. In comparison to right atrial clamping, the R–L shunt flows were higher than the L–R shunt flows. Thus, because the muscular ridge may act as a barrier for right atrial inflow and because the CP is weaker than the CA, it seems that R–L shunts are more likely to occur than L–R shunts.

The *in situ* perfused heart preparation allows for exquisite experimental control of haemodynamics variables that are difficult to manipulate *in vivo* (Perry and Farrell, 1989). However, in spite of these advantages, the *in situ* perfusion differs from *in vivo* conditions. First, outflow pressures are static and the steady decline in central vascular blood pressures that normally occur during diastole does not take place. Therefore, the ventricular valves of the *in situ* perfused heart open later in systole than they would *in vivo*. This is particularly relevant to the pulmonary circulation because diastolic pressure in the pulmonary artery is lower than the systemic arteries, which, even at homogeneous intraventricular pressures causes an earlier opening of the pulmonary arterial valves compared with the systemic valves (e.g. Johansen, 1959). Second, the flows into the left and right atria do not necessarily match  $\dot{Q}_{\text{pul}}$  and  $\dot{Q}_{\text{sys}}$  in the perfused heart, as they would do *in vivo*. Thus, until *in vivo* measurements of flow and pressure relationships are conducted, predictions of *in vivo* shunt patterns of *Python* remain speculative. However, it is unlikely that  $P_{\text{pul}}$  ever exceed  $P_{\text{sys}}$  to the extent that was manipulated in the present study and therefore the R–L shunt is likely to be relatively small.

### Conclusions and perspectives

The *in situ* perfused heart of *Python molurus* exhibits differences in the power development between the systemic and pulmonary circulations, and the cavum arteriosum can generate higher pressures than the cavum pulmonale. Coupled with the marked flow separation, it is likely that *Python molurus* can maintain high systemic blood pressures while having a low blood pressure in the pulmonary circulation to protect against pulmonary oedema (Burggren, 1982). Within non-crocodilian reptiles, considerable ventricular flow and pressure separation have, so far, been documented only in varanid lizards (Burggren and Johansen, 1982). These lizards are characterised by high aerobic metabolic rates and a reduced R–L shunt (and associated improvement of arterial oxygen delivery), as well as the ability to maintain high systemic pressures, which seem imperative to secure sufficient oxygen delivery (Wang and Hicks, 1996; Wang et al., 2001c). *Python molurus* is characterised by an exceptionally large metabolic response to digestion (e.g. Secor and Diamond, 1995) and it is possible that the ventricular separation of *Python molurus* has

evolved in response to the need of maintaining high oxygen delivery during the post-prandial period.

T.W. is in receipt of a Rømer Research Associate Professor fellowship from the Danish Research Council; J.A. is in receipt of a EU postdoctoral fellowship (TMR Contract ERBFMBICT982940) and M.A. is supported by the Swedish Research Council.

### References

- Burggren, W. W.** (1977). Circulation during intermittent lung ventilation in the garter snake *Thamnophis*. *Can. J. Zool.* **55**, 1720–1725.
- Burggren, W. W.** (1982). Pulmonary blood plasma filtration in reptiles: a 'wet' vertebrate lung? *Science* **215**, 77–78.
- Burggren, W. W. and Johansen, K.** (1982). Ventricular hemodynamics in the monitor lizard *Varanus exanthematicus*: pulmonary and systemic pressure separation. *J. Exp. Biol.* **96**, 343–354.
- Farrell, A. P., Davie, P. S., Franklin, C. E., Johansen, J. A. and Brill, R. W.** (1992). Cardiac physiology in tunas. 1. In vitro perfused heart preparations from yellowfin and skipjack tunas. *Can. J. Zool.* **70**, 1200–1210.
- Farrell, A. P., Franklin, C. E., Arthur, P., Thorarensen, G. H. and Cousins, K. L.** (1994). Mechanical performance of an *in situ* perfused heart from the turtle *Chrysemys scripta* during normoxia and anoxia at 5 °C and 15 °C. *J. Exp. Biol.* **191**, 207–229.
- Farrell, A. P., Gamperl, A. K. and Francis, T. B.** (1998). Comparative aspects of heart morphology. In *Biology of Reptilia, Morphology G, Visceral Organs* (ed. C. Gans and A. S. Gaunt), pp. 375–424. Ithaca, NY: SSAR Press.
- Franklin, C. E.** (1994). Intrinsic properties of an *in situ* turtle heart (*Emydera signata*) preparation perfused via both atria. *Comp. Biochem. Physiol.* **107A**, 501–507.
- Franklin, C. E. and Axelsson, M.** (1994). The intrinsic properties of an *in situ* perfused crocodile heart. *J. Exp. Biol.* **186**, 269–288.
- Guyton, A. C.** (1986). *Textbook of Medical Physiology*. Philadelphia: W. B. Saunders.
- Heisler, N. and Glass, M. L.** (1985). Mechanisms and regulation of central vascular shunts in reptiles. In *Cardiovascular Shunts* (ed. K. Johansen and W. W. Burggren), pp. 334–353. Copenhagen: Munksgaard.
- Heisler, N., Neumann, P. and Maloiy, G. M. O.** (1983). The mechanism of intracardiac shunting in the lizard *Varanus exanthematicus*. *J. Exp. Biol.* **105**, 15–31.
- Hicks, J. W.** (1998). Cardiac shunting in Reptiles: mechanisms, regulation, and physiological functions. In *Biology of Reptilia*, Vol. 19: *Morphology G: Visceral Organs* (ed. C. Gans and A. S. Gaunt), pp. 425–483. Ithaca, NY: SSAR Press.
- Hicks, J. W. and Malvin, G. M.** (1995). Mechanisms of intracardiac shunting in reptiles: pressure vs washout shunting. *Adv. Comp. Env. Physiol.* **13**, 73–157.
- Hicks, J. W., Ishimatsu, A., Molloy, S., Erskin, A. and Heisler, N.** (1996). The mechanism of cardiac shunting in reptiles: a new synthesis. *J. Exp. Biol.* **199**, 1435–1446.
- Johansen, K.** (1959). Circulation in the three-chambered snake heart. *Circ. Res.* **7**, 828–832.
- Johansen, K. and Burggren, W. W.** (1980). Cardiovascular function in the lower vertebrates. In *Hearts and Heart-like Organs*, Vol. 1 (ed. G. H. Bourne), pp. 61–117. New York: Academic Press.
- Millard, R. W. and Johansen, K.** (1974). Ventricular outflow dynamics in the lizard, *Varanus niloticus*: responses to hypoxia, hypercarbia and diving. *J. Exp. Biol.* **60**, 871–880.
- Overgaard, J., Busk, M., Hicks, J. W., Jensen, F. B. and Wang, T.** (1999). Acid–base status and arterial oxygen transport following feeding in the snake *Python molurus*. *Comp. Biochem. Physiol.* **124A**, 361–367.
- Perry, S. F. and Farrell, A. P.** (1989). Perfusion preparations in comparative physiology. In *Techniques in Comparative Respiratory Physiology: An Experimental Approach* (ed. C. R. Bridges and P. J. Butler). *Society of Experimental Biology Seminar Series* **37**, 223–257.
- Reeves, R. B.** (1963). Energy costs of work in aerobic and anaerobic turtle heart muscle. *Am. J. Physiol.* **205**, 17–22.

- Secor, S. M. and Diamond, J.** (1995). Adaptive responses to feeding in Burmese pythons: pay before pumping. *J. Exp. Biol.* **198**, 1313–1325.
- Secor, S. M., Hicks, J. W. and Bennett, A. F.** (2000). Ventilatory and cardiovascular responses of pythons (*Python molurus*) to exercise and digestion. *J. Exp. Biol.* **203**, 2447–2454.
- Shelton, G. and Burggren, W. W.** (1976). Cardiovascular dynamics of the Chelonia during apnoea and lung ventilation. *J. Exp. Biol.* **64**, 323–343.
- Strobeck, J. E. and Sonnenblick, E. H.** (1986). Myocardial contractile properties and ventricular performance. In *The Heart and Cardiovascular System* (ed. H. A. Fozzard, E. Haber, R. B. Jennings, A. M. Katz and H. E. Morgan), pp. 31–49. New York: Raven Press.
- Van Mierop, L. H. S. and Kutsche, L. M.** (1985). Some aspects of comparative anatomy of the heart. In *Cardiovascular Shunts* (ed. K. Johansen and W. W. Burggren), pp. 38–56. Copenhagen: Munksgaard.
- Wang, T. and Hicks, J. W.** (1996). The interaction of pulmonary ventilation and the right-left shunt on arterial oxygen levels. *J. Exp. Biol.* **199**, 2121–2129.
- Wang, T., Axelsson, M., Jensen, J. and Conlon, J. M.** (2000). Cardiovascular actions of python bradykinin and substance P in the anesthetized python, *Python regius*. *Am. J. Physiol.* **279**, R531–R538.
- Wang, T., Taylor, E. W., Andrade, D. and Abe, A. S.** (2001a). Autonomic control of heart rate during forced activity and digestion in the snake *Boa constrictor*. *J. Exp. Biol.* **204**, 3553–3560.
- Wang, T., Busk, M. and Overgaard, J.** (2001b). The respiratory consequences of feeding in amphibians and reptiles. *Comp. Biochem. Physiol.* **128A**, 533–545.
- Wang, T., Warburton, S. J., Abe, A. S. and Taylor, E. W.** (2001c). Vagal control of heart rate and cardiac shunts in reptiles: Relation to metabolic state. *Exp. Physiol.* **86**, 777–786.
- Webb, G. J. W.** (1979). Comparative cardiac anatomy of the reptilia III. The heart of crocodylians and an hypothesis on the completion of the interventricular septum of crocodylians and birds. *J. Morph.* **161**, 221–240.
- White, F. N.** (1968). Functional anatomy of the heart of reptiles. *Am. Zool.* **8**, 211–219.